arXiv:1402.7057v1 [cond-mat.stat-mech] 27 Feb 2014

# Layered Percolation

Saikat Guha[1], Donald Towsley[2], Çağatay Çapar[2], Ananthram Swami[3], Prithwish Basu[1]
[1]*Raytheon BBN Technologies, Cambridge, MA 02138,*
[2]*University of Massachusetts, Amherst, MA 01003,*
[3]*US Army Research Laboratory, Adelphi, MD 20783*

We study the emergence of long-range connectivity in multilayer networks (also termed multiplex, composite and overlay networks) obtained by merging the connectivity subgraphs of multiple percolating instances of an underlying backbone network. Multilayer networks have applications ranging from studying long-range connectivity in a communication or social network formed with hybrid technologies, a transportation network connecting the same cities via rail, road and air, in studying outbreaks of flu epidemics involving multiple viral strains, studying temporal flow of information in dynamic networks, and potentially in studying conductivity properties of graphene-like stacked lattices. For a homogenous multilayer network—formed via merging $M$ random site-percolating instances of the same graph $G$ with single-layer site-occupation probability $q$—we argue that when $q$ exceeds a threshold $q_c(M) = \Theta(1/\sqrt{M})$, a spanning cluster appears in the multilayer network. Using a configuration model approach, we find $q_c(M)$ exactly for random graphs with arbitrary degree distributions, which have many applications in mathematical sociology. For multilayer percolation in a general graph $G$, we show that $q_c/\sqrt{M} < q_c(M) < \sqrt{-\ln(1-p_c)}/\sqrt{M}, \forall M \in \mathbb{Z}^+$, where $q_c$ and $p_c$ are the site and bond percolation thresholds of $G$, respectively. We show a close connection between multilayer percolation and mixed (site-bond) percolation, since both provide a smooth bridge between pure-site and pure-bond percolations. We find excellent approximations and bounds on layered percolation thresholds for regular lattices using the aforesaid connection, and provide several exact results (via numerical simulations), and a specialized bound for the multilayer kagome lattice using a site-to-bond transformation technique.

PACS numbers: 03.67.Hk, 03.67.Pp, 04.62.+v
Keywords: percolation, networks, multilayer graph

Percolation theory plays a central role in the study of the sudden formation of a spanning cluster in a large network when a local control parameter $q$ is increased beyond a certain threshold $q_c$. Two popular percolation models refer to $q$ being the probability that a site (or a bond) in the network is occupied. In this case, $q_c$ is known as the site (or bond) percolation threshold, which depend on the network's topology. The evaluation of $q_c$ and various graph properties such as the cluster size distribution, in the subcritical ($q < q_c$) and supercritical ($q > q_c$) regimes have been widely studied. The site and bond percolation thresholds are known exactly only for a handful of simple regular lattices and certain random graphs.

Percolation theory has found use in problems in diverse fields, such as the Ising model of ferromagnetism, which is closely connected to a correlated bond percolation model [1], study of metal-insulator phase transitions [2], conductivity growth in the super-critical regime [3], network communication theory [4–6], studying fractal dimensions of random networks [7], and in analyzing phase transitions in various systems in condensed matter physics, such as the Ising [2], Potts [8], Bose-Hubbard [9] and Widom-Rowlinson models [10].

Percolation properties have been analyzed for *multi-type* networks where each node belongs to one of several types (or colors), where nodes of each type have distinct occupation probabilities [11, 12]. In the last few years, a related but a different class of networks called *multilayer* (also termed *multiplex* or *composite*) networks has seen a surge of scientific interest [13–17, 19]. A multilayer network is obtained by taking the union of the edge sets of multiple subgraphs (layers) of a common underlying graph, thereby activating the bond between two nodes in the multilayer network only if the nodes are both occupied in at least one common layer (see Fig. 1). One common example to motivate a multilayer network is to think of a social network structure with many modes (layers) of social interactions (such as Facebook, Twitter, etc.) between people (nodes) within the same population, where information can traverse the network via a multi-hop flow through nodes that are active in multiple layers, and can thus act as gateways from one layer to another. Other examples of multilayer networks include transportation networks formed by merging individual networks of different means of transportation such as road, rail and air connecting a set of cities, a collection of airline-alliance networks such as Star Alliance and One World, a network of scientific collaborators

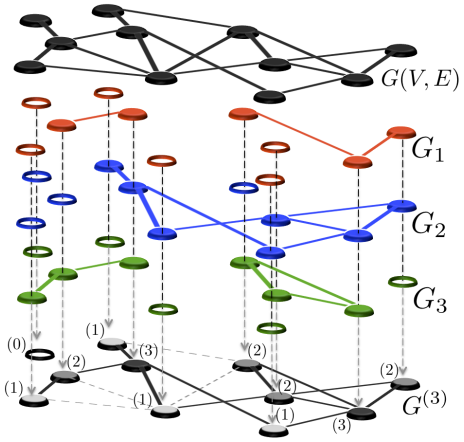


FIG. 1: A multilayer network with $M = 3$ layers.

publishing in different journals, a hybrid communication network over WiFi and cellular technologies, and SIR networks used in epidemic spread studies where an infected carrier may carry multiple viral strains.

In recent years, various studies of multilayer networks were reported, such as their diffusion dynamics [13], cascading failures [14], spectral properties [15], robustness analysis stemming from overlapping multilayer links [16], growing random multilayer networks [17], epidemic spread in overlay networks [18], and a tensorial formulation of multilayer networks [19]. In this paper, we study the connectivity of multilayer networks. We investigate the emergence of long-range connectivity in a multilayer network formed by merging the connectivity graphs of several random site-percolating instances of a network in their sub-critical regimes. One question of interest is: *How sub-critically connected can each layer be while ensuring that long-range connectivity just begins to emerge in the multilayer network?* We address this question by establishing tight scaling laws, analytical bounds, and exact results (via numerical simulation). We study regular two-dimensional grids, as well as random graphs with arbitrary degree distributions. In the case of a multilayer social network for instance, our results can predict what fraction of users need to be active on any one social network, such that a multilayer social network is long-range connected (even though no single social network may be fully connected). We also study the size of the spanning cluster in the multilayer-supercritical regime as a function of the node-density of the individual networks. Furthermore, our analytical characterization of the multilayer configuration model for random graphs could provide a useful tool for analyzing a wide variety of properties of multilayer random graphs, with applications in subfields of mathematical sociology and epidemiology.

## I. LAYERED PERCOLATION

An example construction of a multilayer graph is shown in Fig. 1. Let us consider a graph $G(V, E)$ over a set of sites (or nodes) $V$ and bonds (or edges) $E$. Let us generate $M$ subgraphs $G_i(V, E_i) \subset G$, $1 \leq i \leq M$ by $M$ independent random site-percolation processes on $G$, with site-occupation probabilities, $q_i$. In other words, each layer $G_i$ is formed by *occupying* each site $v \in V$ independently with probability $q_i$, and activating the bonds between all nearest-neighbor occupied sites. The multilayer graph $G^{(M)}(V, E^{(M)}) = \cup_{i=1}^{M} G_i(V, E_i)$ is then formed by taking the union of the bonds of $G_i$. Therefore, bonds $e \in E^{(M)}$ in $G^{(M)}$ will exist only between those nearest-neighbor sites in $G(V, E)$ that are occupied in at least one common layer. When $G$ is a lattice, the multilayer graph can also be visualized as a three-dimensional lattice, a prismatoid with $M$ congruent faces, where the vertical bonds can connect all occupied sites in the $M$ layers in one column. One could construct multilayer graphs in other ways, depending upon the application. Consider for instance a slight change to the connectivity rule described above, where we now *stack* the layers instead of *merging* them, i.e., we connect a node only across adjacent layers if occupied in both layers (instead of connecting each node $v \in V$ across all layers in which $v$ is occupied). This would generate a 3D *stacked* network, percolation properties of which have also been recently studied [20]. Given the more constrained connectivity rule to generate a stacked multilayer graph as compared to a merged multilayer graph, it is evident that the threshold value $q_c$ for the single-layer site-occupation probability for the respective multilayer networks to percolate, will be higher for the former. For instance, as we will show below for the (merged) multilayer square grid, $q_c(M) \sim 1/\sqrt{2M}$ for $M$ large, whereas for the (stacked) multilayer square grid, $q_c(M) \to 0.3116$ for $M$ large—the site-percolation threshold of the 3D simple cubic lattice (see Fig. 3). There could be more complicated connectivity rules in constructing multilayer networks driven by application-specific constraints such as technology compatibility (in a hybrid communication network), hierarchy of information flow (such as in military networks) [21], or causality of information flow, such as in a dynamic network. The last example results in a multilayer *stacked* network with directed bonds connecting nodes across adjacent layers, where the layers correspond to time-snapshots of a temporally evolving network.

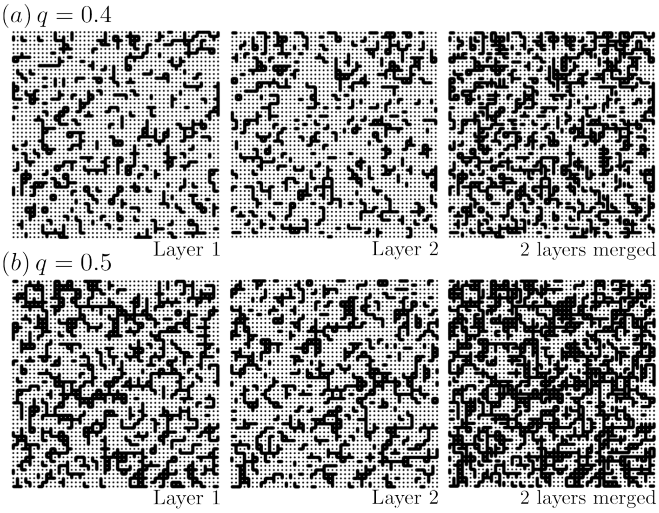


FIG. 2: Merging two site-percolating layers of a square grid ($q_c(1) \approx 0.59$, $q_c(2) \approx 0.47$). (a) At site-occupation probability $q = 0.4 < q_c(2) < q_c(1)$, neither the single layer, nor the two-layer networks have a spanning cluster. (b) At $q = 0.5 > q_c(2)$, the single-layer networks have no spanning cluster, but the two-layer grid has a spanning cluster spanning roughly 65% of the entire network (see Fig. 3(a)).

### A. Results and bounds for arbitrary multilayer networks

In this section, we prove a few upper and lower bounds for multilayer percolation in arbitrary graphs, and use them to prove the asymptotic behavior of $q_c(M)$. Throughout this paper, we will use the variable $q$ (or, $Q$) to denote site-occupation probability, and $p$ (or, $P$) for bond-occupation probability. Let us first consider the following theorem on homogenous mul-

tilayer bond percolation, where 'homogenous' refers to the fact that the bond (or site) occupation statistics are taken to be identical in each network layer.

**Theorem 1** *For a homogenous multilayer network formed via merging $M$ random bond-percolating instances of the same graph $G$ with bond-occupation probability $p$, the threshold $p_c(M)$ on the single-layer bond-occupation probability such that a spanning cluster appears in the multilayer network is given by, $p_c(M) = 1 - (1 - p_c)^{1/M} \to [-\ln(1 - p_c)]/M$ as $M \to \infty$, where $p_c$ is the bond-percolation threshold of $G$.*

**Proof.** The proof follows from the simple observation that the multilayer network is equivalent to a simple bond percolation process on $G$ with bond-occupation probability $1 - (1 - p)^M$. ∎

Next, we show an upper and a lower bound on $q_c(M)$ for homogenous multilayer site percolation.

**Theorem 2** *For a homogenous multilayer network formed via merging $M$ random site-percolating instances of the same graph $G$, the following upper bound holds for the threshold on the single-layer site-occupation probability $q$, $q_c(M) \leq \sqrt{1 - (1 - p_c)^{1/M}}$ such that a spanning cluster appears in the $M$-layer network, where $p_c$ is the bond-percolation threshold of $G$.*

**Proof.** Consider a bond $B$ in the multilayer graph $G^{(M)}$, and the corresponding bonds $B_1, \ldots, B_M$ in the $M$ respective layers. Consider the two sites $u_i$ and $v_i$ at the two end points of $B_i$, $1 \leq i \leq M$. Each of these $2M$ sites is occupied independently with probability $q$. Therefore, $P[B \text{ is occupied}] = 1 - (1 - q^2)^M \equiv p$. The bonds in $G^{(M)}$ can be thought of as generated by a positively-correlated bond-percolation process with a uniform marginal bond-occupation probability $p$. Hence, $p > p_c$ is sufficient for a spanning cluster to appear in $G^{(M)}$ where $p_c$ is the bond percolation threshold of the underlying network $G$ (note that $p \geq p_c$ may not be necessary for multilayer percolation due to the positively-correlated bond process). It thus follows that $q \geq \sqrt{1 - (1 - p_c)^{1/M}}$ is sufficient for percolation. Therefore the multilayer threshold must satisfy, $q_c(M) \leq \sqrt{1 - (1 - p_c)^{1/M}}$. ∎

**Proposition 3** *For a homogenous multilayer network formed via merging $M$ random site-percolating instances of the same graph $G$, $q_c(M) \geq \sqrt{1 - (1 - q_c^2)^{1/M}}$, where $q_c \equiv q_c(1)$ is the site-percolation threshold of $G$.*

**Proof.** We provide only a semi-rigorous proof for this proposition in see Appendix A, which uses a connection between layered percolation and mixed (site-bond) percolation. We also evaluate a rigorous lower bound to $q_c(M)$ for the kagome lattice using Scullard's star-triangle transformation technique [32] (see Appendix C for details), which provide further evidence to this proposition. ∎

**Lemma 4** *It follows readily from Theorem 2 and Proposition 3, that $q_c(M) = \Theta(1/\sqrt{M})$.*

**Proof.** First note that the upper bound in Theorem 2 can be further upper bounded as, $q_c(M) \leq \sqrt{1 - (1 - p_c)^{1/M}} < \sqrt{-\ln(1 - p_c)}/\sqrt{M}, \forall M$, where the second inequality can be shown to be asymptotically tight as $M \to \infty$. Similarly, note that the lower bound in Proposition 3 can be further lower bounded as, $q_c(M) \geq \sqrt{1 - (1 - q_c^2)^{1/M}} > q_c/\sqrt{M}, \forall M$. Combining the two, we have the matching lower and upper bounds,

$$q_c/\sqrt{M} < q_c(M) < \sqrt{-\ln(1 - p_c)}/\sqrt{M}, \ \forall M \in \mathbb{Z}^+. \quad (1)$$

∎

Since the second upper bound in the proof of Lemma 4 is asymptotically tight w.r.t. the upper bound in Theorem 2, and as evidenced by empirical results to be shown in Section I B, we conjecture the following convergence property for $q_c(M)$:

**Conjecture 5** *For a homogenous multilayer network formed via merging $M$ random site-percolating instances of the same graph $G$, the threshold on the single-layer site-occupation probability for the $M$-layer network to percolate, $q_c(M)$ satisfies, $\lim_{M\to\infty} q_c(M)/\left[\sqrt{-\ln(1 - p_c)}/\sqrt{M}\right] = 1$.*

Finally, note that with successive layers being merged into one, the average cluster sizes will grow with the number of layers $M$. Hence, intuitively, the single-layer site-occupation probability $q$ at which the $M$-layer network should percolate (have a spanning cluster appear) should decrease as $M$ increases. The following monotonicity property on $q_c(M)$ makes this intuition precise.

**Proposition 6** *$q_c(M)$ is a non-increasing function of $M$, i.e., $q_c(M) \geq q_c(M + 1), \forall M$.*

**Proof.** This is easily proven using sample path arguments. Given a site-occupation probability $q$ for each of $M$ layers, the addition of an additional $(M + 1)$-st layer with the same site-occupation prbability can only increase the number of connected sites. Consequently, if a spanning cluster appears in the network with site-occupation probability $q$, then it can only increase in size with the additionof the $(M + 1)$-st layer. One practical import of this is that we can limit our search for $q_c(M + 1)$ to the interval $(0, q_c(M)]$. ∎

### B. Layered percolation on regular lattices

Newman and Ziff introduced an efficient Monte Carlo algorithm for studying site or bond percolation on any lattice [26], which runs essentially in linear time. This algorithm has been extensively used since then for numerical analyses of percolating systems, and extended to analyzing random graphs [27], continuum percolation on an Eulidean space [28], and interconnected networks [20]. We used a variation of the Newman-Ziff algorithm (details in Appendix B) to simulate multilayer percolation for several 2D regular lattices—the square, triangular, Archimedian and kagome lattices.

Simulation results on a $512 \times 512$ square grid are summarized in Fig. 3. The size of the spanning cluster (in terms of the fraction of nodes in the entire network) is shown in

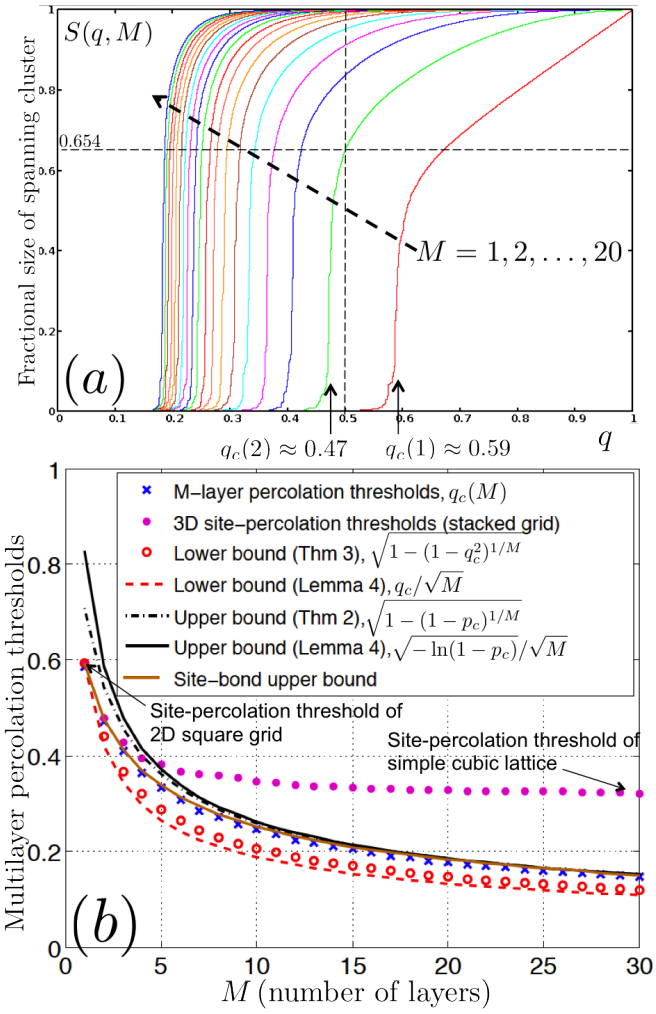


FIG. 3: (Color online) Thresholds and bounds for the multilayer square lattice. Simulations performed on a 262144 node lattice.

Fig.3(a) for $M = 1, \ldots, 20$ layer lattices, as a function of the single-layer site-occupation threshold, $q \in [0,1]$. Fig. 2 shows explicitly how two site-percolating layers of a square grid are merged to obtain a two-layer network. For the square grid, $q_c(1) \approx 0.59$ and $q_c(2) \approx 0.47$. In Fig. 2, note that at $q = 0.4 < q_c(2) < q_c(1)$, neither the single layer, nor the two-layer networks have a spanning cluster, whereas at $q = 0.5 > q_c(2)$, the single-layer networks have no spanning cluster, but the two-layer grid has a spanning cluster. When the grid is large, this cluster should span roughly 65% of the entire network as predicted by the $M = 2$ plot in Fig. 3(a). In Fig. 3(b), the (blue) crosses show the multilayer thresholds $q_c(M)$ for the square grid obtained via simulations. The (black) dash-dotted line is upper bound from Theorem 2 and the (red) circles plot the lower bound from Proposition 3.

We also studied multilayer percolation on the kagome lattice. Our results are summarized in Fig. 4(a). Aside from the numerics, we developed a lower bound for $q_c(M)$ specifically for the kagome lattice, leveraging a technique developed by Scullard [32]. It is a site-to-bond transformation technique

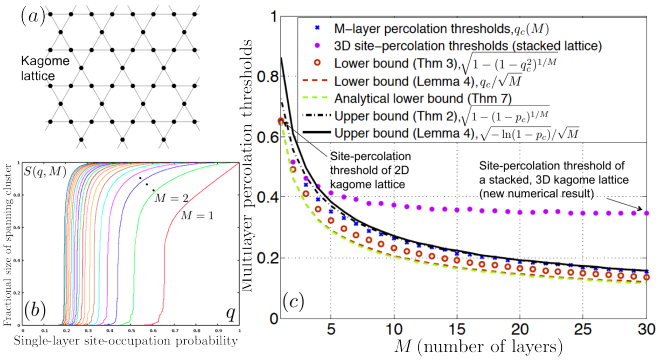


FIG. 4: (Color online) Thresholds and bounds for the multilayer kagome lattice. Simulations performed on a 196608 node lattice.

that leverages the duality of the triangular and honeycomb lattices to compute the critical surface for any correlated bond percolation process on the triangular lattice where the correlations are limited to within each triangular face. He further used a clever decoupling construction to use the above technique to exactly compute the site-percolation threshold of the kagome lattice, as $q_c = 1 - 2\sin\pi/18 \approx 0.6527$. Using a similar technique (See Appendix C for details), we evaluated a lower bound to the multilayer site percolation threshold for the kagome lattice, which is tantalizingly close to the lower bound from Lemma 4, $q_c(1)/\sqrt{M}$, but the two are not exactly equal (see Fig. 4(c)). The lower bound found using the Scullard technique is given as follows.

**Theorem 7** *For the kagome lattice, $q_c(M) \geq q_{LB,\,Kagome}(M)$ for $M \geq 1$, where $q_{LB,\,Kagome}(M)$ is the unique root of the following polynomial $f_M(q)$, in $[0,1]$:*

$$\begin{aligned} f_M(q) &= [(1-q)(1+q-q^2)]^M + 2(1-2q^2+q^3)^M \\ &- [(1-q)^2(1+2q)]^M - (1-q^2)^M - Mq^2. \end{aligned} \quad (2)$$

**Proof.** See Appendix C. ∎

A by-product of our simulations—that of the 3D stacked Kagome lattice (which is of great interest due to its interesting magnetic properties [30, 31])—is the numerical evaluation of the site-percolation threshold of the 3D stacked Kagome lattice, $q_{c,\text{stacked}} \approx 0.366$, which we believe has not been reported elsewhere (see the magenta dots in Fig. 4(c)).

## II. EXACT RESULTS FOR RANDOM GRAPHS

In this section, we will study layered percolation on random graphs with an arbitrary degree distribution. This model of random graph analysis—based on a probability-generating function (PGF) approach—was developed by Newman *et al.* [33], and is known as the *configuration model* (CM). The CM has found use in modeling several real life networks that have non-Poisson distributions, such as the truncated power-law and exponential distributions [26].

### A. Thresholds: characterization and convergence

Let $p_k$ denote the probability that a randomly selected node has degree $k$. Let $\mathcal{M}$ denote the set of $M$ layers and let $q_k$ denote the probability that a vertex of degree $k$ is occupied in layer $m \in \mathcal{M}$. As before, the events that a node is occupied in different layers are assumed to be independent. $p_k(1-(1-q_k)^m)$ is the probability of a node having degree $k$ and being occupied in at least one layer, and

$$F_0(x) = \sum_{k=0}^{\infty} p_k(1-(1-q_k)^M)x^k$$

is the PGF of this distribution. Let us follow a randomly chosen edge $e(u,v)$ starting from a node $u$, occupied in $n \leq M$ layers, to node $v$. Node $v$ has degree distribution proportional to $kp_k$ [26]. Thus the PGF of the distribution of $v$ having degree $k$ *and* being occupied in at least one of $n$ layers that $u$ is occupied in, is given by

$$F_n(x) = \frac{\sum_{k=1}^{\infty} kp_k(1-(1-q_k)^n)x^{k-1}}{z},$$

for $1 \leq n \leq M$, where $z = \sum_k kp_k$ is the average node degree.

Let $H_0(x)$ denote the PGF of the cluster size that a randomly selected node belongs to. It is easy to argue that,

$$H_0(x) = 1 - F_0(1) + x\sum_{k=0}^{\infty} p_k \sum_{l=1}^{M} \binom{M}{l} q_k^l (1-q_k)^{M-l} H_l(x)^k.$$

Let us define $H_n(x)$ as the PGF for the size of a cluster that a neighbor of the node belongs to provided that it is occupied in at least one of the $n$ layers in which the randomly selected node is occupied in. It is given by,

$$H_n(x) = 1 - F_n(1) + x\sum_{k=1}^{\infty} \frac{kp_k}{z} \times \sum_{l=1}^{M} \left[\binom{M}{l} - \binom{M-n}{l}\right] q_k^l (1-q_k)^{M-l} H_l(x)^{k-1}$$

where $\binom{j}{i}$ is defined to be zero whenever $i > j$. The combinatorial term in the inner sum corresponds to the number of combinations of $l$ layers at a neighbor that overlap the $n$ layers of the original node. When $l > M-n$, all possible combinations of $l$ layers at the neighbor overlaps the $n$ layers in the original node, yielding $\binom{M}{l}$ whereas when $l \leq M-n$, we have to subtract out the number of $l$ layer combinations that do not overlap the $n$ layer combinations at the original node, $\binom{M-n}{l}$. We are interested in the average cluster size that a randomly selected node belongs to, which is given by $\mu_0 = H_0'(1)$,

$$\mu_0 = F_0(1) + x\sum_{k=0}^{\infty} kp_k \sum_{l=1}^{M} \binom{M}{l} q_k^l (1-q_k)^{M-l} \mu_k, \qquad (3)$$

where $\mu_n = H_n'(1)$, i.e.,

$$\mu_n = F_n(1) + \sum_{k=1}^{\infty} \frac{(k-1)kp_k}{z} \times \sum_{l=1}^{M} \left[\binom{M}{l} - \binom{M-n}{l}\right] q_k^l (1-q_k)^{M-l} \mu_l.$$

Consider the case $q_k = q$. We introduce the matrix $\mathbf{A} = [A_{ij}]$ with

$$A_{ij} = \begin{cases} -C\left(\binom{M}{j} - \binom{M-i}{j}\right) q^j (1-q)^{M-j} & i \neq j \\ 1 - C\left(\binom{M}{j} - \binom{M-i}{j}\right) q^j (1-q)^{M-j} & i = j \end{cases}$$

where $C = \sum_k (k-1)kp_k/z$. Now $\mu = (\mu_1, \ldots, \mu_M)$ is the solution of

$$\mathbf{A}\mu^T = \mathbf{b}^T, \qquad (4)$$

where $\mathbf{b} = (F_1(1), \ldots F_M(1))$. We define the critical occupancy probability, $q_c(M)$, such that when $q > q_c(M)$, there exists one (infinite size) spanning cluster w.h.p., and when $q < q_c(M)$, there exist only finite size clusters.

**Proposition 8** *For a random graph, $q_c(M)$ is the unique solution of:*

$$\det(\boldsymbol{A}(q)) = 0 \qquad (5)$$

*within the interval* $[0,1]$.

**Proof.** The size of a spanning cluster, or a giant-connected component, is a constant fraction of the size of the network. Hence, for an infinite random graph, appearance of a spanning cluster in the $M$-layer network is equivalent to $\mu_0$ diverging (to infinity). As Eq. (3) shows, $\mu_0$ is a constant plus a linear combination of $\{\mu_k\}$, $k = 1, \ldots, M$. Hence, at least one element of $\mu$ must diverge for $\mu_0$ to diverge. Since $\boldsymbol{b}$ is a constant vector, this can only happen if $\boldsymbol{A}$ is singular. ∎

For the case $M = 1$, this corresponds to finding the solution of $q - C = 0$, which yields the known result $q_c = 1/C$ [33]. For the case of $M = 2$, $q_c$ is the unique solution of the following polynomial

$$C^2q^4 - C^2q^3 - Cq + 1 = 0 \qquad (6)$$

within the interval $[0,1]$, which is

$$q_c(2) = \frac{1}{4}\left[a + 1 - \sqrt{3 + 2a - a^2}\right], \qquad (7)$$

with $a = \sqrt{1 + 8/C}$.

It is easy to show that there exists at least one real root in the interval $[0,1]$ provided that $C > 1$ as $\det(\mathbf{A}(0)) = 1$ and $\det(\mathbf{A}(1)) = 1 - C < 0$. Numerically, it is easy to verify that there is a unique root of $\det(\mathbf{A}(0)) = 1$ for all $M \geq 1$ as long as $C > 1$.

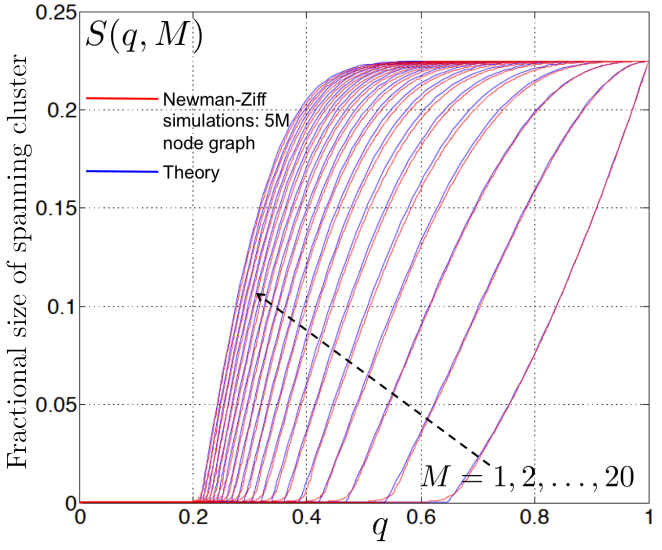


FIG. 5: Size of the spanning cluster for multilayer percolation as a function of the single-layer site-occupation probability $q$ for a random graph with a truncated power law node-degree distribution; $p_k = 0, k = 0$, $p_k = Ck^{-\tau}e^{-k/\kappa}, k \geq 1$, with $\kappa = 10$ and $\tau = 2.5$. The theory plots were obtained by solving Eqs. (8) and (9). The numerical plots were obtained by Newman-Ziff style simulations, via averaging over 10 instances of a 5 million node random graph.

### B. Largest cluster size

In the supercritical regime, the fractional size of the giant connected component is given by $S = 1 - H_0(1)$. For the $M$-layer random graph, $S(q, M)$ is given by

$$S(q, M) = 1 - (1-q)^M - \sum_{k=0}^{\infty} p_k \sum_{l=1}^{M} \binom{M}{l} q^l (1-q)^{M-l} u_l^k, \quad (8)$$

where $\boldsymbol{u} = [u_1, u_2, \ldots, u_M]^T \in [0, 1]^M$ is given by the following self-consistency matrix equality:

$$\boldsymbol{u} = \boldsymbol{s} + \boldsymbol{B}\boldsymbol{v} \quad (9)$$

where $s_l = (1-q)^l$, $v_l = f(u_l) \equiv \sum_{k=1}^{\infty} (kp_k/z) u_l^{k-1}$, and $B_{ij} = \left[\binom{M}{j} - \binom{M-i}{j}\right] q^j (1-q)^{M-j}$.

### C. Results

In order to test our theory, we performed numerical simulations of layered site percolation on random graphs with up to $M = 20$ layers, and 5 million nodes, and compared with results obtained from the theory we developed above. We chose random graphs with node degrees distributed according to the truncated power law [27],

$$p_k = \begin{cases} 0 & \text{for } k = 0, \\ Dk^{-\tau}e^{-k/\kappa} & \text{for } k \geq 1, \end{cases} \quad (10)$$

where $D = \left[\mathrm{Li}_\tau(e^{-1/\kappa})\right]^{-1}$ is a normalization constant, with the polylogarithm function, $\mathrm{Li}_s(x) \equiv \sum_{k=1}^{\infty} x^k/k^s$. We chose this distribution for our simulations since it is seen in a number of real-world social networks including collaboration networks of movie actors [34] and scientific collaborations based on co-authorship of publications [35]. The pure power-law distributions seen in Internet data are also included as a special case $\kappa \to \infty$.

For our numerical evaluations of $q_c(M)$, we used the Newton-Raphson method to extract the unique root of Eq. (5). In order to solve for the largest cluster size $S(q, M)$, we solved Eq. (9) numerically using a multi-dimensional iterative fixed-point method to search for the unique solution of $\boldsymbol{u} \in [0, 1]^M$. One interesting thing to note is that the multilayer threshold $q_c(C, M)$ is only a function of $C \equiv \sum_{k=1}^{\infty}(k-1)kp_k/z$, regardless of the actual distribution $\{p_k\}$ (see Fig. 6(a)).

The evaluations of the largest cluster size $S(q, M)$ as a function of the single-layer site-occupation probability $q$—both using the theoretical formulation in Sections II A and II B, as well as using efficient Newman-Ziff style Monte-Carlo simulations on random graph instances with 5 million nodes—for a truncated power law node-degree distribution, with $\kappa = 10$ and $\tau = 2.5$, are summarized in Fig. 5. Excellent agreement is seen between theory and numerical simulations.

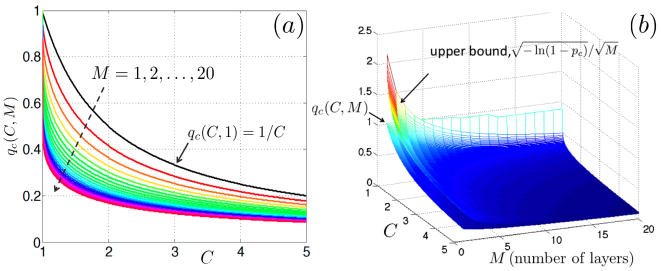


FIG. 6: (Color online) (a) The multilayer threshold $q_c(C, M)$ as a function of $C$ for $M = 1, 2, \ldots, 20$ layers. (b) Comparing $q_c(C, M)$ with the general upper bound derived in Lemma 4. The random graphs used for these evaluations were chosen from a truncated power law node-degree distribution (10), with $\kappa = 10$ and $\tau = 2.5$.

## III. SITE-BOND AND LAYERED PERCOLATION

Joint *site-bond* percolation is a well-studied extension of site and bond percolation [23–25], in which sites are occupied independently with probability $Q$, and each bond is occupied independently with a probability $P$. In the *site-and-bond* variation of site-bond percolation, a path or a cluster can be formed using occupied sites *and* occupied bonds. So, all bonds that do not have both sites at their ends occupied, can be ignored without loss of generality. In other words, an equivalent way to generate a site-bond percolating graph would be to first occupy all sites independently with probability $Q$, and then for each bond connecting a pair of occupying sites, flip a $(P, 1-P)$ biased coin to decide whether to turn that bond active. The question is what is the region in the $(P, Q)$ space where percolation happens? $P = 1, Q \geq Q_c$ and $Q = 1, P \geq P_c$ correspond to pure-site and pure-bond percolation regions, shown by the blue and red lines in Fig. 7

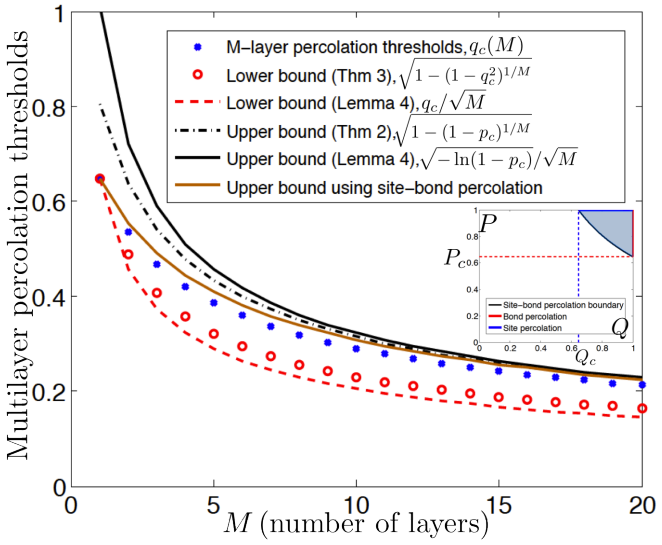


FIG. 7: Upper and lower bounds on the multilayer site-percolation thresholds for a random graph with a truncated power law degree distribution (10), with $\kappa = 10$ and $\tau = 2.5$. The exact $q_c(M)$ values were obtained by solving Eq. (5), which also match very well with the simulation results in Fig. 6.

inset. The shaded region in that figure is the percolating region, whose boundary is not known exactly for any lattice. For a random graph with an arbitrary degree distribution $\{p_k\}$, it is easy to derive, using the machinery in Ref. [27], that the site-bond percolation boundary is given by $PQ \geq 1/C$, where $C = \sum_k (k-1)kp_k/z$, with $z = \sum_k kp_k$. Now, we are ready to prove the following upper bound for layered percolation in a random graph.

**Theorem 9** *For multilayer site-percolation on a random graph with degree distribution $\{p_k\}$, the M-layer thresholds $q_c(M) \leq q_{\mathrm{UB,Random-Graph}}$, where $q_{\mathrm{UB,Random-Graph}}$ is the unique root of the following polynomial $g_M(q)$, in $[0,1]$:*

$$g_M(q) = (1-q^2)^M - \frac{1}{C}(1-q)^M + (1/C) - 1. \qquad (11)$$

**Proof.** As we noted in the discussion following Proposition 3, the multilayer graph can be thought of being generated by a site-bond percolation process, where sites are independently occupied with probability $Q = 1-(1-q)^M$, and conditioned on two nearest-neighbor sites being both occupied, the bond between them is occupied with probability $P = \left[1-(1-q^2)^M\right] / \left[1-(1-q)^M\right]^2$. In other words, $P$ is the probability that two sites are occupied in at least one common layer, given they are both occupied. For a single layer, $P = 1$ correctly reduces to pure-site percolation. For $M > 1$, there is a problem: the multilayer construction generates a site-bond process as described above, but with the bond occupation probabilities having (positive) spatial correlations. In other words, if we are considering three consecutive occupied sites $u$, $v$ and $w$, then the event that the $u-v$ bond exists, conditionally *increases* the probability that the $v-w$ bond exists. This means that if we solve for $q$ by setting $PQ = 1/C$ (this gives us Eq. (11)), we will get an upper bound, $q^*(M) \geq q_c(M)$, on the true thresholds, the reason being that percolation will happen sooner in the actual multilayer random graph due to the positive bond correlations. ■

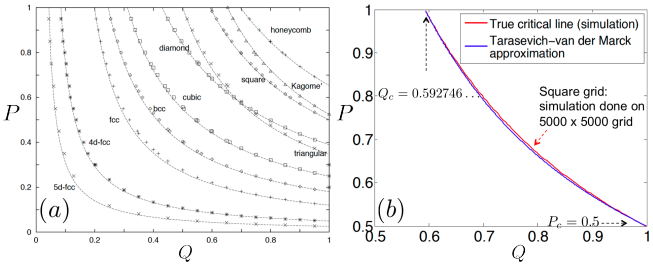


FIG. 8: Site-bond critical regions: comparison between true critical region and the Tarasevich-van der Marck approximation, (a) Figure from Ref. [25], (b) Refined simulations for the critical region for square grid using Newman-Ziff method on a 25-million-node grid.

Note that $q^*(1) = q_c(1)$, by definition. So, unlike the upper bounds in Theorem 2 and Lemma 4, this upper bound is tight at $M = 1$, and as shown in Fig. 7, the site-bond upper bound is the tightest of all upper bounds to $q_c(M)$.

Yanuka and Englman proposed an approximation to that boundary for general lattices [24], which was later improved by Tarasevich and van der Marck [25], who showed that the site-bond critical region for any lattice is well-approximated by $P(Q+A) = B$, with $A = (P_c - Q_c)/(1-P_c)$ and $B = P_c(1-Q_c)/(1-P_c)$. We present their results in Fig. 8(a), and refine their simulations via the Newman-Ziff method for the square-grid, plotted in Fig. 8(b). The approximations of the $P-Q$ critical line results may suggest that once the pure site and pure bond thresholds $Q_c$ and $P_c$ are known for any lattice, the entire critical curve is fixed, i.e., there is no need for additional parameters such as critical exponents, dimension, or coordination number, to describe the critical curve. This is however not true. As we noted above however, for random graphs with arbitrary degree distributions, no parameters other than $P_c = Q_c = 1/C$ are needed to characterize the critical line $PQ = 1/C$. Last year, some semi-analytical progress was reported for the triangular lattice [36]. The problem of finding the real law for the critical line remains unsolved. However, seeing how well the Tarasevich-van der Marck approximation tallies with the true site-bond critical line (Fig. 8), it is evident that inverting them would give us good approximations to the multilayer thresholds. We thus have the following proposition.

**Proposition 10** *The multilayer threshold $q_c(M)$ for any network $G$ is well-approximated by the unique solution to the following polynomial equation in $q$, in the interval $[0,1]$:*

$$\left[1-(1-q^2)^M\right]\left[1-(1-q)^M + a\right] = b\left[1-(1-q)^M\right]^2,$$

*where $a = (p_c - q_c)/(1-p_c)$ and $b = p_c(1-q_c)/(1-p_c)$ are constants that depend upon the site and bond percolation thresholds $q_c$ and $p_c$ of $G$, respectively.*

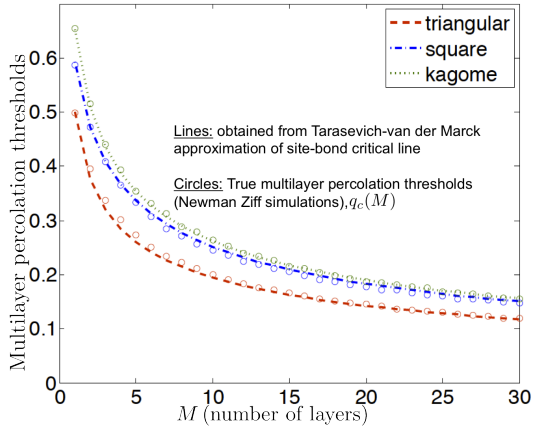


FIG. 9: Comparison of true multilayer thresholds—for the square, triangular and kagome lattices—to approximations obtained by inverting the Tarasevich-van der Marck approximations to the site-bond critical line for a general graph.

**Remark 11** *Using the same argument as in Theorem 9, the intersection of the true site-bond critical line with* $PQ^2 = 1 - (1 - q^2)^M$ *yields a strict* upper bound *to* $q_c(M)$. *We used the simulation results in Fig. 8(b) to compute an upper bound to* $q_c(M)$ *for the square lattice, which is shown (light brown plot) in Fig. 3 to be extremely close to the true thresholds.*

Fig. 9 shows the agreement of the approximations with the true thresholds $q_c(M)$ for the square, triangular and kagome lattices. Note that the approximations are neither an upper nor a lower bound to $q_c(M)$ in general, but they are better approximations compared with any of the formal bounds we reported earlier in this article, and will likely be so for many other lattices, as evidenced by the results from [25] in Fig. 8(a).

## IV. CONCLUSIONS

Multilayer networks come about by merging multiple subgraphs of an underlying backbone network. Each subgraph (layer) may represent a distinct mode of communication (such as center-frequencies in a multi-radio network), different overlaying social networks in a given population, networks of distinct means of transportation connecting a set of cities, time snap shots of an evolving network topology, or even layers of a stacked lattice such as graphene. Multilayer networks have a broad range of applications that range from studying long-range connectivity in hybrid communication, social, or transportation networks, in studying outbreaks of epidemics that may involve multiple viral strains, studying temporal flow of information in dynamic networks, and potentially in studying electrical conductivity of stacked lattices.

In this paper, we studied the connectivity of multilayer networks. We proved several upper and lower bounds on $q_c(M)$, the threshold value of the single-layer site-occupation probability that determines when a spanning cluster begins to emerge in an $M$-layer network. We developed an analytical framework based on the configuration model, with which we derived the thresholds $q_c(M)$ exactly for random graphs with arbitrary degree distributions. These random graphs have been extensively studied to model real-life social networks such as collaboration networks of researchers and movie actors. We also found a close-relationship between layered percolation and joint site-bond percolation, a fairly well-studied topic, and translated a known good approximation to the site-bond critical line for a wide class of graphs, to a good approximation on multilayer connectivity thresholds. Both our random graph analysis, as well as the relationship with site-bond percolation could find use in several future directions of research in multilayer networks.

Depending upon the application, different aspects of multilayer networks may play an important role. Our work focused on connectivity. But one could look into a variety of other aspects. For connectivity purposes we treated all occupied edges equally, but edges that are active on more layers could be more robust to failures, have lower resistivity in a conductivity analysis of a stacked lattice, or be able to bear a higher throughput in a hybrid communication network. Furthermore, for ease of analysis, we assumed the underlying population for generating each layer, to be the same. This may not be true in a real-life multilayer network. One could look into a variety of alternative connectivity models to construct multilayer networks driven by the application, such as compatibility across communication modes or technologies, information traversal hierarchy (such as in military networks), causality of information flow (such as in a temporally evolving network) where the vertical axis in Fig. 1 is time, or stacked lattices (where nodes can connect across one or two nearest layers). Finally, it would be very interesting to analyze multilayer versions of the SIR model of epidemic spread, such as analyzing vaccination strategies with limited supplies when nodes can carry multiple viral strains.

### Acknowledgments

SG thanks Hari Krovi for useful discussions. Research was sponsored by the Army Research Laboratory and was accomplished under Cooperative Agreement Number W911NF-09-2-0053 (the ARL Network Science CTA). The views and conclusions contained in this document are those of the authors and should not be interpreted as representing the official policies, either expressed or implied, of the Army Research Laboratory or the U.S. Government. The U.S. Government is authorized to reproduce and distribute reprints for Government purposes notwithstanding any copyright notation here on. CC acknowledges support from the NSF grant CNS-1018464.

[1] C.-K. Hu, Physical Review B, **29**, 9 (1984).

[2] M. Walther, D. G. Cooke, C. Sherstan, M. Hajar, M. R. Free-

man, and F. A. Hegmann, Physical Review B, **76**, 125408 (2007).
[3] Nicolas Posé, N. A. M. Araújo, and H. J. Herrmann, Physical Review E, **86**, 051140 (2012).
[4] M. Franceschetti, O. Dousse, D. N. C. Tse, and P. Thiran, IEEE Transactions on Information Theory, **53**, No. 3, March (2007).
[5] W. Ren, Q. Zhao, and A. Swami, IEEE Transactions on Information Theory, **57**, 7, 4315–4332, July (2011).
[6] S. Guha, P. Basu, C.-K. Chau, and R. Gibbens, IEEE Journal on Selected Areas in Communications (JSAC), **29**, No. 8, September (2011).
[7] R. Cohen, and S. Havlin, Physica A **334**, 6–13, (2004).
[8] F. Y. Wu, Journal of Statistical Physics, **18**, 2, (1978).
[9] A. Niederle, and H. Rieger, New Journal of Physics, **15**, 075029 (2013).
[10] J. T. Chayes, L. Chayes, and R. Kotecký, Communications of Mathematical Physics, **172**, 551–569 (1995).
[11] B. Söderberg, Physical Review E 66, 066121 (2002).
[12] A. Allard, P.-A. Noël, Louis J. Dubé, and Babak Pourbohloul, Physical Review E **79**, 036113 (2009).
[13] S. Gómez, A. Díaz-Guilera. J. Gómez-Gardeñes, C. J. Pérez-Vicente, Y. Moreno, and A. Arenas, Physical Review Letters **110**, 028701 (2013).
[14] J. Gao, S. V. Buldyrev, H. E. Stanley, Xiaoming Xu, and Shlomo Havlin, Physical Review E, **88**, 062816 (2013).
[15] A. S.-Ribalta, M. D. Domenico, N. E. Kouvaris, A. Diaz-Guilera, S. Gómez, and A. Arenas, Physical Review E, **88**, 032807 (2013).
[16] D. Cellai, E. López, J. Zhou, J. P. Gleeson, and Ginestra Bianconi, Physical Review E, **88**, 052811 (2013).
[17] V. Nicosia, G. Bianconi, V. Latora, and M. Barthelemy, Physical Review Letters, **111**, 058701 (2013).
[18] V. Marceau, P.-A. Noël, L. H.-Dufresne, A. Allard, and L. J. Dubé, Physical Review E, **84**, 026105 (2011).
[19] Manlio De Domenico, Albert Solé-Ribalta, Emanuele Cozzo, Mikko Kivelä, Yamir Moreno, Mason A. Porter, Sergio Gómez, and Alex Arenas, Physical Review X, **3**, 041022 (2013).
[20] K. J. Schrenk, N. A. M. Araujo, and H. J. Herrmann, Physical Review E, **87**, 032123 (2013).
[21] P. Basu, C.-K. Chau, R. Gibbens, S. Guha, and R. Irwin, Proceedings of the 11th International Symposium and Workshops on Modeling and Optimization in Mobile, Ad Hoc and Wireless Networks (WiOpt), May 13-17, (2013).
[22] J. M. Hammersley, Journal of Mathematical Physics, **2**, 728–733 (1961).
[23] J. M. Hammersley, Mathematical Proceedings of the Cambridge Philosophical Society, **88**, 167–170, DOI:10.1017/S0305004100057455, (1980).
[24] M. Yanuka, R. Englman, Journal of Physics A: Math. Gen. **23** L339 (1990).
[25] Y.Y. Tarasevich, S.C. van der Marck, International Journal of Modern Physics C **10**, 1193 (1999).
[26] M. E. J. Newman and R. M. Ziff, Physical Review Letters, **85**, 4104 (2000).
[27] D. S. Callaway, M. E. J. Newman, S. H. Strogatz, and D. J. Watts, Physical Review Letters, **85**, 25 (2000).
[28] S. Mertens and C. Moore, Physical Review E, **86**, 061109 (2012).
[29] J. Wang, Z. Zhou, W. Zhang, T. M. Garoni, and Y. Deng, Physical Review E, **87**, 052107 (2013).
[30] D. P. Kozlenko, A. F. Kusmartseva, E. V. Lukin, D. A. Keen, W. G. Marshall, M. A. de Vries, and K. V. Kamenev, Physical Review Letters, **108**, 187207 (2012).
[31] W.-S. Wang, Z.-Z. Li, Y.-Y. Xiang, and Q.-H. Wang, Physical Review B **87**, 115135 (2013).
[32] C. R. Scullard, Physical Review E, **73**, 016107 (2006).
[33] M. E. J. Newman, S. H. Strogatz, and D. J. Watts, Physical Review E, **64**, 026118 (2001).
[34] L. A. N. Amaral, A. Scala, M. Barthélémy, and H. E. Stanley, Proc. Natl. Acad. Sci. U.S.A. **97**, 11149 (2000).
[35] M. E. J. Newman, Proc. Natl. Acad. Sci. USA **101**, 5200–5205 (2004).
[36] M.I. González, P. Centres, W. Lebrecht, A. J. Ramirez-Pastor, F. Nieto, Physica A, **392**, 6330–6340 (2013).
[37] E. Tarjan, Journal of the Association for Computing Machinery, **22**, No. 2, 215–225 (1975).
[38] D. Achlioptas, R. M. D'Souza, J. Spencer, Science, **323**, No. 5920, 1453–1455 (2009).
[39] A. Coniglio, H.E. Stanley, W. Klein, Physical Review Letters, **42**, 518 (1979).

## Appendix A: Mixed percolation and a lower bound on multilayer percolation thresholds

### 1. Introduction

Mixed percolation (also known as *site-bond percolation*) bridges between pure-site and pure-bond percolation. As we showed in Eq. (1), layered percolation provides yet another bridge between pure-site percolation (single layer) to pure-bond percolation (many layers). So, it is not surprising that these two problems should be related to one another. Site-bond percolation was first introduced by Hammersley [22] as a process where sites and bonds are independently occupied, and a path can only traverse through occupied sites *and* occupied bonds. Among several applications, this was used to describe the sol-to-gel transition (gelation) of polymers [39]. In this model, bonds represent chemical bonds, occupied sites represent monomers, and empty sites represent solvent molecules.

In site-bond percolation, each site is independently occupied with probability $Q$, and each bond is independently occupied with probability $P$. Note that one can equivalently define $P$ to be the conditional probability of activating the bond in between two sites, conditioned on both sites being occupied (this does not change the definition, since activated bonds that do not have both sites at their end points occupied, do not contribute to creating a cluster). The site-bond *critical line* connects the pure-site percolation threshold $Q_c$ to the pure-bond percolation threshold $P_c$ of the same graph (see the solid black line in Fig. 10).

Since the site and bond percolation thresholds themselves are not known for a majority of lattices and random graphs, calculating the exact site-bond critical line is even harder. However, some important properties of the critical line are known [23], and some excellent approximations to the critical line have been found [24, 25], which are functions only of the site and bond percolation thresholds of the underlying graph, $Q_c$ and $P_c$, respectively.

### 2. Some properties of site-bond percolation

Let $\mathcal{P}(Q, P)$ denote the percolation probability, i.e., the probability that a randomly chosen vertex in the graph belongs to an infinite-size (spanning) cluster. The site-bond critical line is where $\mathcal{P}(Q, P)$ transitions from 0 (to its left) to 1 (to its right). See Fig. 10. Hammersley showed that [23],

$$\mathcal{P}(q\lambda, p) \le \mathcal{P}(q, p\lambda), \tag{A1}$$

for $0 \le q \le p \le 1$, and $0 \le \lambda \le 1$. This shows that along any hyperbola $PQ = c$ (the red dashed lines in Fig. 10), where $c \in (0, 1)$ is a constant, the percolation probability $\mathcal{P}(Q, P)$ must increase from top to bottom (i.e., from $(c, 1)$ to $(1, c)$). This in turn implies that the value of $PQ$ must *decrease* along any constant-$\mathcal{P}$ line. The critical line is the only constant-$\mathcal{P}$ line shown in Fig. 10, but one could imagine plotting several such lines at different $\mathcal{P}$ values, each of which will cross the

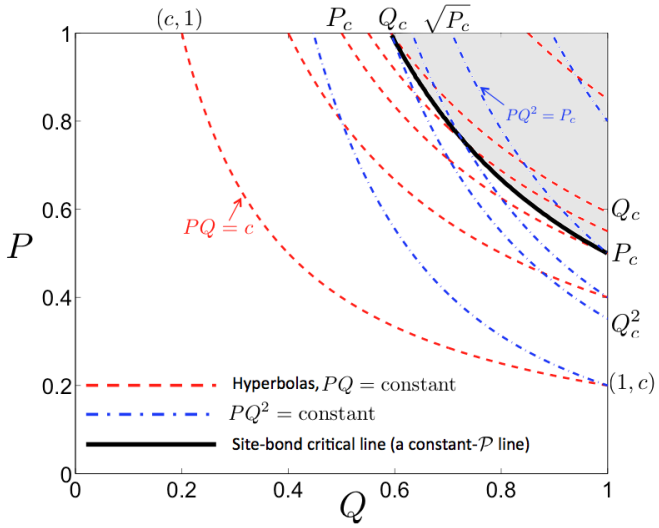


FIG. 10: Site-bond percolation on a square lattice. The critical line (solid black plot) was obtained via Newmann-Ziff style simulation of site-bond percolation on a square grid with 25 million nodes. The shaded area shows the percolating region.

hyperbolas ($PQ = c$) from high to low $c$ values. So, the family of constant-$\mathcal{P}$ lines are 'steeper' than the hyperbolas. Next, let us note that since $PQ$ is constant along each hyperbola, $PQ^2$ must increase along any hyperbola (going from top to down), as $Q$ increases. On the other hand, since $PQ$ decreases along a constant-$\mathcal{P}$ line, whereas $Q$ increases, it is not immediately clear whether $PQ^2$ should increase or decrease. Finally, note that since $Q_c^2 < P_c$ for any graph, the constant-$PQ^2$ line $PQ^2 = P_c$ must lie above the critical line, and the constant-$PQ^2$ line $PQ^2 = Q_c^2$ must lie below the critical line. So, the constant-$PQ^2$ lines are even 'steeper' than the constant-$\mathcal{P}$ lines. Therefore, by continuity, $PQ^2$ must decrease along a constant-$\mathcal{P}$ line, and in particular along the site-bond critical line. Hence, we have the following proposition:

**Proposition 12** *For site-bond percolation on any graph $G$, where each site is occupied independently with probability $Q$, and each bond is occupied independently with probability $P$, the marginal probability of a bond (or the fraction of bonds occupied) $PQ^2$, monotonically increases along the critical line, form $Q_c^2$ to $P_c$. Furthermore, $PQ^2$ monotonically increases along any constant-$\mathcal{P}$ locus in the site-bond plane, going from the pure-site to the pure-bond percolation limits.*

Note that the argument above does *not* constitute a formal mathematical proof of Proposition 12.

The fraction of occupied bonds (or, the marginal probability of any single bond) at the threshold of pure-bond percolation is $P_c$, whereas it is $Q_c^2$ at the threshold of pure-site percolation. It is well known that $Q_c^2 \le P_c$ in general. The intuitive reason for this is that site-percolation can be seen as a correlated bond percolation process, where the (positive) correlations between neighboring bond occupations cause a spanning cluster to appear with a smaller fraction of bonds in the graph, than the fraction of bonds that would need to be occupied if they

were activated independently. Stated in a different way, for the same marginal probability of a bond, the percolation probability $\mathcal{P}$ (the probability that a spanning cluster exists) is higher when the bonds are spatially (positively) correlated. Proposition 12 essentially states that this transition of the marginal probability of a bond (at the percolation threshold) increases monotonically along the critical line, from its pure-site value $Q_c^2$ to its pure-bond value $P_c$.

### 3. A lower bound to the multilayer percolation threshold

We are now ready to prove Proposition 3, restated below:

**Proposition 13** *For a homogenous multilayer network formed via merging $M$ random site-percolating instances of the same graph $G$, $q_c(M) \geq \sqrt{1-(1-q_c^2)^{1/M}}$, where $q_c \equiv q_c(1)$ is the site-percolation threshold of $G$.*

**Proof.** The multilayer graph can be thought of as being generated by a correlated site-bond process, where sites are independently occupied with probability $Q = 1-(1-q)^M$, and conditioned on two nearest-neighbor sites being both occupied, the bond between them is occupied with probability $P = \left[1-(1-q^2)^M\right] / \left[1-(1-q)^M\right]^2$. $P$ is the probability that the two sites are occupied in at least one common layer, given they are both occupied. For a single layer (i.e., $M = 1$), we have $P = 1$, which reduces to pure site percolation. Therefore using Proposition 12, we have that the marginal probability of a bond at the multilayer percolation threshold ($PQ^2$, at $q = q_c(M)$) should be no smaller than $q_c(1)^2$, the pure site percolation threshold of the underlying graph $G$. Therefore we have,

$$1-(1-q_c(M)^2)^M \geq q_c(1)^2, \tag{A2}$$

which yields, $q_c(M) \geq \sqrt{1-(1-q_c^2)^{1/M}}$, $q_c \equiv q_c(1)$. ∎

### 4. Discussion

There is one subtle difference between standard site-bond percolation and multilayer percolation. It is that the nearest neighbor bonds are a little more correlated in multilayer percolation as compared to site-bond percolation. The reason for this is that given three successive sites on a path are occupied, in the standard $(P, Q)$ site-bond process, the probability of both bonds to be occupied is $P^2$, whereas in multilayer percolation (with $P$ and $Q$ defined as above), the probability of both bonds to be occupied (conditioned on all three sites being occupied) is greater than $P^2$. This is the reason why the true site-bond critical line—when 'translated' to multilayer percolation, yields a strict upper bound to the multilayer thresholds, $q_c(M)$. The brown solid lines in Fig. 3(b) and Fig. 7 plot this upper bound. Note that this bound, unlike the upper bound from Theorem 2, is tight both at $M = 1$ and $M \gg 1$, since it interpolates between pure-site and pure-bond processes, which is a characteristic of both multilayer percolation and site-bond percolation. This is why the upper bound is very close to the true multilayer thresholds. Similarly, the exact multilayer thresholds, when translated to the site-bond plane, should yield a good, and strict lower bound to the site-bond critical line.

Finally, note that Proposition 12 can be proven rigorously based on our arguments above, if we replace the exact site-bond line with the shifted-hyperbola approximations of Tarasevich *et al.* [25], which are known to have excellent agreement with the true site-bond critical lines on a large class of lattices (see Fig. 8(a), which was borrowed from [25]).

## Appendix B: Newman-Ziff simulations of layered percolation

In order to run multilayer simulations on lattices and random graphs, we used an adaptation of the Newman-Ziff technique [26]—an efficient algorithm to simulate site and/or bond percolation systems whose runtime is essentially linear (in the number of nodes or sites). Let us first review the basic algorithm.

### 1. The Newman-Ziff algorithm

The underlying idea is based on a union-find algorithm [37]. One chooses a random order in which sites (or bonds) are occupied sequentially, and the algorithm keeps track of all the connected components at each step using a union-find data structure. Each cluster is represented by one *root* member, and every member $i$ is linked to a unique parent $p(i)$ in the same cluster as $i$, except the roots who are their own parents. There are two main functions: `findroot(i)` and `merge(i,j)`. `findroot(i)` follows the links (viz., $p(p(i))\ldots$) from $i$ to the root of its cluster, $r(i)$. Every time a new member $i$ is added to the percolating system, the algorithm iterates through all nearest neighbors of the new member, and for each neighbor $j$ that is occupied, it calls the `merge(i,j)` routine, which uses `findroot(i)` and `findroot(j)` to find $r(i)$ and $r(j)$ and declares the one whose cluster is larger to be the parent of the other (viz., $p(r(i)) = r(j)$ if $i$'s cluster is smaller than $j$'s), unless of course $r(i) = r(j)$ in which case they are already in the same cluster. The runtime of `findroot(i)` is proportional to the length of the path from $i$ to $r(i)$, which an inductive argument shows can never exceed $\log_2 N$, where $N$ is the system size. Newman-Ziff used a trick called *path compression* to make these paths—averaged over the execution of the algorithm—even smaller. When `findroot(i)` traces its way to $r(i)$, noting that $r(i)$ is the root for each object $j$ along the path from $i$ to $r(i)$, it assigns $p(j) = r(i)$ for all those objects, linking each one directly to the root of the cluster. So next time we call `findroot`, it would work in a single step. With this modification to `findroot()`, the amortized cost of the `findroot` and `merge` operations (cost per operation, averaged over many operations), is *essentially* $O(N)$. To be precise, the amortized cost per step is proportional to the inverse of the Ackermann function $\alpha(N)$, which grows incredibly slowly with $N$ [37].

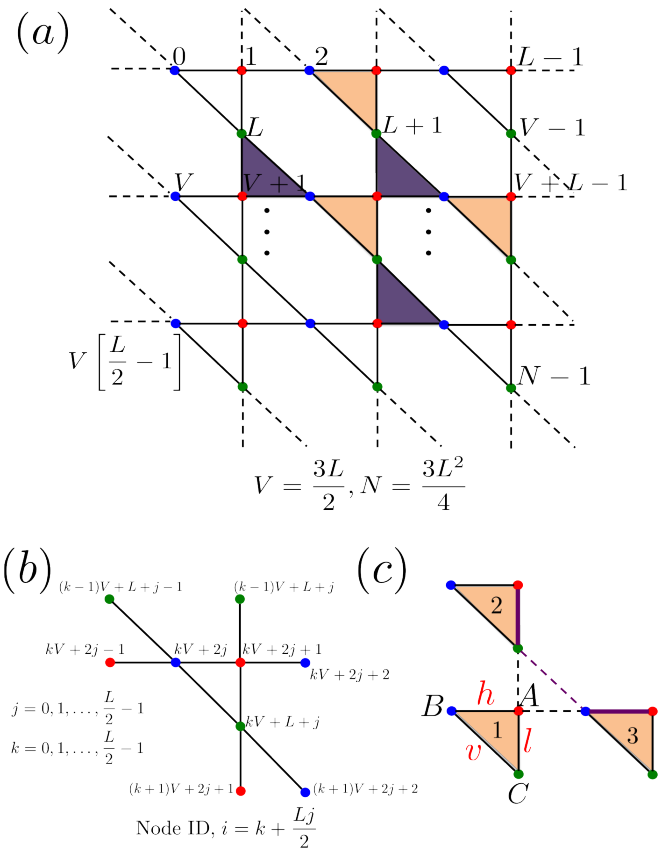


FIG. 11: (a) Casting the Kagome lattice in the square grid, with one of every 4 nodes in the grid removed. The dashed edges are ones that 'wrap around'. (b) A 'unit cell' of the Kagome lattice showing the three node *types*, and also the node numbering convention we use to construct the nearest-neighbor matrix for use in the layered grid connectivity simulations. (c) Scullard's setup for calculating the critical region for correlated-bond percolation on a triangular lattice, with bond correlations limited within each face.

### 2. Simulation of layered percolation

The first step in setting up the simulation for layered percolation is to create the nearest-neighbor matrix $A$, where $A(i,k) = j$ means node $j$ is the $k$-th neighbor of node $i$, $1 \le k \le d(i)$, where $d(i)$ is the degree of node $i$. As an illustration of the construction of the nearest-neighbor matrix, we show in Fig. 11 how we numbered the nodes for the Kagome lattice, and assigned values to $A(i,k)$ for $0 \le i \le N-1$, $0 \le k \le 3$, for a Kagome lattice with $N$ nodes each of degree, $d = 4$.

Algorithm 1 summarizes the remainder of the algorithm MultiLayerNewmannZiff$(A, N, M)$, that takes as inputs, the nearest-neighbor matrix $A$, the number of nodes $N$ and the number of layers $M$, and produces estimates of the multilayer thresholds, $q_c(m)$, $m = 1, \ldots, M$. The algorithm, as written below, accurately estimates the sizes of the largest cluster, ClusterSize$(m,i)$ for an $m$-layer merged lattice as a function of the single-layer site-occupation probability, $q \equiv i/N$. For lattices, the maximum cluster sizes ClusterSize$(m,i)$ have a sharp discontinuity at $q = q_c(m)$ (i.e., $i = i_c \equiv Nq_c(m)$) for an infinite size lattice (see Fig. 3(a) for instance), for $N$ large enough. Therefore, the $i$ value where the discrete slope of the maximum cluster size (ClusterSize$(m,i)$ − ClusterSize$(m,i-1)$) is maximum gives a pretty good estimate of $i_c(m)$ (hence, that of $q_c(m)$), which suffices for the purposes of this paper. A more accurate way to estimate the threshold $q_c(m)$ involves estimating the *wrapping probabilities*, which are probabilities that a cluster wraps around the lattice boundary conditions, either vertically, or horizontally, or both. For details, see Ref. [26].

### Appendix C: Derivation of the Kagome lattice lower bound

In this appendix, we will derive a lower bound on $q_c(M)$ stated in Theorem 7, which is reproduced below:

**Theorem 14** *For the kagome lattice, $q_c(M) \ge q_{LB,\ Kagome}(M)$ for $M \ge 1$, where $q_{LB,\ Kagome}(M)$ is the unique root of the following polynomial $f_M(q)$, in $[0,1]$:*

$$\begin{aligned} f_M(q) &= [(1-q)(1+q-q^2)]^M + 2(1-2q^2+q^3)^M \\ &- [(1-q)^2(1+2q)]^M - (1-q^2)^M - Mq^2. \end{aligned} \quad \text{(C1)}$$

**Proof.** The derivation of this bound uses a technique introduced by Scullard [32], who developed a site-to-bond transformation technique that leverages the duality of the triangular and honeycomb lattices to compute the critical surface for any correlated bond percolation process on the triangular lattice where the correlations are limited to within each triangular face [32]. Fig. 11(c) shows the setup. Imagine a triangular lattice formed by the shaded triangular faces, and for a moment ignore the dashed lines connecting the faces (i.e., collapse the three dashed lines into one node). The purpose of the dashed lines is to depict that there are no (bond or site existence) correlations in between faces. However, within each face, could there be a very complex correlated bond or site percolating network (but that network must be identical from face to face). Scullard showed that the critical condition for such a correlated-triangular lattice to percolate is given by the condition $P[A,B,C] = P[\bar{A},\bar{B},\bar{C}]$, where $P[A,B,C]$ is the probability that all three end nodes of a face are connected, and $P[\bar{A},\bar{B},\bar{C}]$ is the probability that none of the three nodes are connected to one another. A special case of this is that of correlated bond percolation, where each face has just three bonds $AB \equiv h$, $BC \equiv v$, and $CA \equiv l$, whose occupation probability is given by the joint distribution $P(h,v,l)$. The percolation condition for this case translates to:

$$P(v) + P(\bar{v},h,l) = P(\bar{h},\bar{l}). \quad \text{(C2)}$$

Scullard then observed that one way to generate such a correlated bond percolation on the triangular lattice—but one where the correlations do not traverse the lattice faces—is to consider a pure site percolating kagome lattice as shown in Fig. 11(a), where all the orange (light) shaded triangles are the faces of a triangular lattice where the faces are detached from one another via the dashed lines as shown in Fig. 11(c). If the

site-occupation probability is $q$, it is easy to see that $P(v) = q^2$, $P(\bar{h}, \bar{l}) = (1-q) + q(1-q)^2$, and $P(\bar{v}, h, l) = 0$, substituting which in (C2) yields a solution $q_c = 1 - 2\sin\pi/18 \approx 0.6527$. The last observation to be made is that if these orange (light) shaded triangular faces percolate (meaning there is a spanning cluster involving adjoining light-shaded faces), all the dashed bonds in Fig. 11(c) in that spanning cluster must also be occupied. Reason being, due to three-point correlations, a dashed bond will be occupied with probability 1 if two bonds on either side of it are open. More specifically, consider the bonds on triangles 2 and 3 in Fig. 11(c). Under the transformation described above, if any one bond in each triangle is occupied, then both bounding sites on each of these bonds will be occupied. But if this is true, then it follows that the dashed bond between triangles 2 and 3 will also be occupied. Thus the two occupied bonds in the faces considered above are connected to one another via the dashed bond, just by virtue of being occupied themselves. Thus, by inserting the separating dashed triangles between the triangular faces, we have preserved the conditions for Eq. (C2) to be valid—that of neighboring triangular faces to be independent. Hence, $q_c = 1 - 2\sin\pi/18$, via this construction, is the pure site percolation threshold of the kagome lattice [32].

Now consider applying the above technique to the $M$-layer merged kagome lattice. We can still use Eq. (C2), but it will only give a necessary condition for the $M$-layer lattice to percolate, since the existence of one bond each in triangles 2 and 3 will no longer necessitate the dashed bond separating them to be occupied, because the end nodes of the dashed line could now be occupied in non-intersecting layer sets. Therefore, the solution to (C2) will yield a lower bound to $q_c(M)$—the minimum value of single-layer site occupation probability such that the $M$-layer lattice will percolate. With a little combinatorics (detailed arguments omitted), one can calculate the following probabilities:

$$P(v) = Mq^2, \tag{C3}$$

$$P(\bar{h}, \bar{l}) = (1-q)^M (1+q-q^2)^M, \text{ and} \tag{C4}$$

$$P(\bar{v}, h, l) = (1-q^2)^M + \left[(1-q)^2(1+2q)\right]^M - 2(1-2q^2+q^3)^M, \tag{C5}$$

substituting which in Eq. (C2), one obtains the condition stated in Theorem 14 to calculate the lower bound, $q_{\text{LB, Kagome}}(M) \leq q_c(M)$. ∎

There are a couple of interesting things to note about this lower bound.

- The lower bound to $q_c(M)$ for the kagome lattice obtained using the Scullard technique is incredibly close to the general lower bound from Lemma 4, $q_c(1)/\sqrt{M}$ (see Fig. 4(c)). But a closer inspection reveals the two are not exactly equal. Indeed, substituting $q_c/\sqrt{M}$ with $q_c = 1-2\sin\pi/18$ into the polynomial $f_M(q)$ in Eq. (C1) results in a number *very close to*, but not exactly zero.

- Another interesting thing to note is that when $q > q_{\text{LB, Kagome}}(M)$, by the Scullard argument, all the orange (light) shaded triangles in the infinite multilayer Kagome lattice (see Fig. 11(a)) will form a spanning cluster amidst themselves, i.e., assuming the purple (dark) shaded triangles do not come in the way of a pair of occupied nearest neighbor light-shaded triangles to get 'connected'. But then, because of symmetry, when $q > q_{\text{LB, Kagome}}(M)$, all the purple (dark) shaded triangles should also have a spanning cluster ('ignoring' the light-shaded triangles). So, when $q$ is in the regime, $q_{\text{LB, Kagome}}(M) < q < q_c(M)$, the light-shaded triangles percolate, *and* the dark-shaded triangles percolate, but the full multilayer Kagome lattice does not percolate, which happens only when $q \geq q_c(M)$. This situation has some semblance with the notion of *explosive percolation*, that has been studied recently [38].

**Algorithm 1** MultiLayerNewmannZiff($A$, $N$, $M$)

**Require:** The nearest-neighbor matrix $A$ of a graph $G$, and the total number of layers, $M$.

**for** $m = 0$ to $M - 1$ **do**
  Initialize: cluster size dummy variable, $C(m) = 0$;
  Generate a random permutation, $\pi_m()$ of $[1, \ldots, n]$;
  **for** $i = 0$ to $N - 1$ **do**
    ptr$(m, i)$=EMPTY;
  **end for**
**end for**
**for** $i = 0$ to $N - 1$ **do**
  **for** $m = 0$ to $M - 1$ **do**
    occupied$(m', \pi_{m'}(i)) = 0$;
    **for** $m' = 0$ to $m$ **do**
      $s_1 = \pi_{m'}(i)$;
      occupied$(m', s - 1) = 1$;
      **if** ptr$(m, s_1) \neq$ EMPTY **then**
        $r_1$ = FindRoot$(s_1, m)$;
        **if** $-$ptr$(m, r_1) >$ big$(m)$ **then**
          big$(m)$= $-$ptr$(m, r_1)$;
        **end if**
      **else**
        ptr$(m, s_1) = -1$;
        $r_1 = s_1$;
      **end if**
      **for** $j = 0$ to $d - 1$ **do**
        $s_2 = A(s_1, j)$;
        **if** occupied$(m', s_2) = 1$ **then**
          $r_2$ = FindRoot$(s_2, m)$;
          **if** $r_2 \neq r_1$ **then**
            **if** ptr$(m, r_1) >$ ptr$(m, r_2)$ **then**
              Increment ptr$(m, r_2)$ by ptr$(m, r_1)$;
              ptr$(m, r_1) = r_2$;
              $r_1 = r_2$;
            **else**
              Increment ptr$(m, r_1)$ by ptr$(m, r_2)$;
              ptr$(m, r_2) = r_1$;
            **end if**
            **if** $-$ptr$(m, r_1) > C(m)$ **then**
              $C(m) = -$ptr$(m, r_1)$;
            **end if**
          **end if**
        **end if**
      **end for**
    **end for**
    ClusterSize$(m, i) = C(m)/N$;
  **end for**
**end for**
**for** $m = 0$ to $M - 1$ **do**
  $\text{slope}_{\max} = 0$;
  **for** $i = 1$ to $N - 1$ **do**
    slope = ClusterSize$(m, i)$-ClusterSize$(m, i - 1)$;
    **if** slope $> \text{slope}_{\max}$ **then**
      $\text{slope}_{\max}$ = slope;
      $q_c(m) = i/N$;
    **end if**
  **end for**
**end for**
**return** multilayer percolation thresholds, $q_c(m)$, $0 \leq m \leq M - 1$.
**function** FindRoot$(i, m)$
  **if** ptr$(m, i) < 0$ **then**
    **return** $i$;
  **end if**
  **return** ptr$(m, i)$ = FindRoot(ptr$(m, i), m)$;
**end function**